Gas flow in a permeable medium

By L. M. de SOCIO and L. MARINO

Department of Mechanics and Aeronautics, University of Rome 'La Sapienza',
Via Eudossiana 18, I-00184 Roma, Italy

The dynamics of gases in permeable media is approached both experimentally and by numerical simulations. The experiments were performed in matrices made of packed beds of spheres in rarefied conditions and a model for the direct simulation of the molecular kinetics is proposed. Comparisons between experimental data and numerical results show the influence of the main parameters of the gas–solid interaction and the range of validity of the model. Moreover it is shown that there is a flow condition for the minimum permeability of the medium to the gas flow. Such a minimum depends upon the Knudsen number, and can be explained by the molecular dynamics as in the well-known Knudsen's experiment on capillaries.

1. Introduction

Recent developments in a number of technological areas require that permeable media, namely porous media, matrices, metallic foams and beds of granular materials, be reconsidered from the point of view of the physics of fluids. This is, for instance, the case of microtechnology devices, boundary-layer control by wall suction, transpiration cooling, controlled combustion, and so on, where the gas flowing through the solid medium is very often in more or less rarefied conditions if one considers the free molecular path of the fluid and the mean diameter of the microchannels through which the gas flows. In this framework, our paper reports the results of a series of experiments on the gas flow through a permeable medium made of a bed of spheres, as this particular geometrical configuration was believed to be the most suitable way to characterize the statistical behaviour of both the gas and the solid phase and was proposed in the past as a reliable model of a porous medium.

The experimental work and a related proposed model for the direct simulation of the flow were aimed at showing and discussing how a physically realistic representation of the gasdynamics in permeable media must rely on the molecular kinetics of fluids, in so overcoming the continuum models which were derived from the Darcy equation for liquids. In particular, the numerical simulations were carried out to explain and substantiate theoretically the experimental data, in regimes from the free molecular flow to the compressible continuum.

As an introduction to the work we briefly recall that M. Knudsen, in a celebrated paper (Knudsen 1909), reported on some experiments concerning the gas flow in capillary tubes, and showed that the flow rate through the capillaries, normalized with respect to the value in the free molecular regime (Karniadakis & Beskok 2001), first decreases, reaches a minimum and thereafter increases with the pressure drop between the two ends of the tube. At that time, the effects of capillarity on liquid flows were already known, but very little was known about gas flows in capillaries. What was more important than the experimental data was the explanation Knudsen

gave of the phenomenon he had observed. Based on the kinetic theory, the minimum normalized flow rate at increasing pressure drops could be argued as the situation, occurring at relatively low pressure, where the gas flow through the tube ceases to be a stream of free molecules which only hit against the wall, and undergoes the increasing effects of the collisions between the molecules. Later Adzumi (1937a, b) predicted a linear influence of the gas rarefaction on the normalized flow rate in an almost continuum regime and this phenomenon was subsequently named the Klinkenberg effect.

It took about fifty years, after Knudsen's observations, before attention was paid to the possibility that similar phenomena might be present in flows through porous media where the mean free path of the streaming molecules is comparable with the mean diameter of the pores (Wicke & Vollmer 1952). Up to that time, the fluid flow through a porous matrix had been described by the Darcy law for liquids or by the modifications and extensions of such a law to gases via a generally phenomenological approach.

We recall here that a widely accepted definition of the medium permeability to gases, which will be used in this paper, can be extended and expressed in the form

$$K_d = up/(|\nabla p|) \quad (\text{m}^2\,\text{s}^{-1}), \tag{1.1}$$

where u and p are the local values of the percolating velocity and of the pressure, respectively, and $|\nabla p|$ is the pressure gradient. Equation (1.1) expresses the isothermal mass flow rate per unit pressure gradient and can be interpreted more as the conductance of the medium rather then its permeability. Actually, the medium permeability to incompressible isothermal fluids, as defined by Darcy, is

$$k = -u/(|\nabla p|/\mu) \quad (\text{m}^2), \tag{1.2}$$

where μ is the viscosity, and its meaning can be recovered easily from (1.1) if we follow, for instance, the demonstration by Wu, Pruess & Persoff (1998).

Let the Darcy law (1.2) be associated to the continuity equation for a compressible, isothermal gas through the pores, with a local average velocity $\bar{U} = u/\varphi$, where φ is the porosity. Then

$$\partial(\rho u)/\partial x = -\varphi \partial \rho/\partial t, \tag{1.3}$$

where ρ is the mass density, t is the time and introducing (1.2) into (1.3) we have

$$\frac{\partial p^2}{\partial t} = K_d \partial^2(p^2)/\partial x^2, \tag{1.4}$$

which shows the physical meaning of $K_d = kp/\varphi\mu$ as representative of the gas diffusivity through the medium.

A few years after the Wicke & Vollmer work, a first study (Derjagin & Bakanov 1957) of gas flows through porous matrices was based on the Boltzmann equation to predict the existence of a minimum of the permeability K_d versus the mean pressure in the medium. Derjagin & Bakanov, in particular, considered the medium as a mixture of gas and solid particles, according to a procedure of the 'dusty gas' type (Muskat 1937).

Pollard & Present (1948) gave a sound theoretical basis to Knudsen's arguments about the flow in capillaries, and Scott & Dullien (1962) predicted a partial extension of those results to the porous solids. However, the first experiments concerning the latter particular point, as reported in Grove & Ford (1958), were not conclusive and left many uncertainties owing to the difficulty of characterizing the tested material, namely porous ceramics and graphites.

At present, a large number of results concerning the gas flows through porous media deal with the prediction of a Klinkenberg effect (Klinkenberg 1941) in these materials. These results are related to the molecular kinetics (see for example Wu *et al.* 1998; Skjetne & Auriault 1999; Chastanet, Royer & Auriault 2004) in the sense that the Navier–Stokes equations for a compressible continuum fluid are solved after assuming the presence of a velocity slip at the interface between gas and porous medium. The slip coefficient appears in the boundary conditions and its value is simply taken from the results of the kinetic theory of gases. Then a linear Klinkenberg law is expressed in the form

$$k = k_0(1 + b/p), \tag{1.5}$$

where b is a gas-dependent constant, and k_0 is the permeability of the porous sample to liquids.

Finally, Gorelik *et al.* (1993) reconsidered the 'dusty gas' model to simulate and solve by a Monte Carlo method the problem of mass transfer through a porous layer in the presence of intense evaporation (condensation). However, in that work, the spheres of the bed are simulated as the immovable particles of a gas mixture, and unrealistic data were assumed for the porosity. This assumption could be justified since the scope of that paper was to present a model for the kinetics of an intense evaporative mass transfer in the layer. Stefanov *et al.* (1999) presented further results about the more complex situation of a mixture of an evaporating component in a porous layer in the presence of a non-condensable gas. In Stefanov *et al.*, the bed of spheres is simply a reference medium for the condensation/evaporation model testing, but no attention is paid to a realistic representation of the medium.

Two main models of a porous medium were followed, in most cases, in order to explain the experimental data from a theoretical point of view. One of them assumes that the medium can be represented as a bundle of capillary tubes (Erofeev, Freedlender & Kogan 1998*a*, *b*) and it follow that the 'Knudsen effect' for its permeability should be recovered. However, no experimental evidence of the validity of this point of the theory was made available, and the deterministic form assumed for the structure of the solid makes the model of little use in providing more information on the gasdynamics of a porous system. In this framework, Marschall & Milos (1998) studied the permeability of some rigid fibrous media in the continuum and slip flow regimes. They showed the analogy between flows in capillary tubes and through permeable materials and gave experimental results concerning the Klinkenberg law for fibrous media in an almost continuum regime.

The second model, which is much more frequently cited (e.g. Bear 1988), deals with a permeable medium as made of a more or less geometrically ordered bed of spheres. In this case, it is less immediate to predict the existence of a Knudsen effect while – to the best of our knowledge – no experimental evidence has been yet presented in the literature.

In the following sections, experimental results on the characteristics of a flow in a permeable medium, made of a compact bed of spheres, will be shown together with the results of the numerical simulations which are first validated by, and then extend, the experiments. An advantage of choosing a bed of spheres as a reference situation is that the main geometrical parameters of this configuration are sufficiently known. Among the results it will be shown that the Knudsen effect is present and that a minimum exists for the medium permeability in (1.1) with the pressure gradient.

A final note concerns the way the experimental data were obtained. In the past, all the results were given in terms of the relation between the flow rate (either through

capillaries or through porous media) and the total pressure drop between the inlet and the outlet of the probe. However, when dealing with gases, the downstream pressure was kept as low as possible, so that, at the exit, choked flow conditions were usually present. It follows that in most cases, the real pressure drop was not correctly evaluated by taking the pressure of the discharge ambient instead of the pressure at the exit section in choked conditions. As a consequence, the considered pressure drops were higher than the actual ones. This fact had further relevant consequences when the mean value of the characteristics of the state of the gas was calculated, e.g. the mean Knudsen number. We overcame these difficulties by taking the measurements along the probe.

2. Experimental rig and results

The experiments were carried out in the Aerodynamics Laboratory of the Department of Mechanics and Aeronautics of the University of Rome 'La Sapienza'. The test section was a stainless steel cylinder, $L = 170 \pm 0.1$ mm long and of internal diameter $D_w = 27 \pm 0.1$ mm, filled with compacted glass spheres, the diameter D_s of which could be 0.5, 1, 2 (± 0.01) mm. The porosity of an indefinite bed of spheres falls in a range between the limits 0.4764, for spheres ordered according to a cubic packing, and 0.2595, for rhombohedral packing (see for example Bear 1988; Dullien 1991). Accurate measurements gave a mean value of the porosity of our probes $\varphi = 0.33$ for all three diameters.

The mean diameter of the pores d_p depends upon the structure of a porous medium. The simplest approximation is the use of the 'hydraulic' diameter of an equivalent circular tube (Dullien 1991) and the ratio d_p/D_s takes the value $1/3$ in the case of spheres of equal diameter. Therefore the ratio between d_p and L is negligible in our case and we can assume that the end effects on the flow are limited to the very short regions close to the inlet and to the outlet of the test probe. In those regions, the value of the porosity presents abrupt changes which are difficult to evaluate. On the other hand, an entrance boundary layer develops at the cylindrical wall, which might play a more and more important role as the gas rarefaction increases. Very close to the wall, the porosity increases owing to the discrepancy between the radii of curvature of the wall and the particles, and the influence of the ratio D_s/D_w is felt for three or four particle diameters into the packing (Dullien 1991). These assumptions will be verified by means of the numerical simulations.

Along the wall of the probe, seven static pressure and two thermocouple holes were opened. The test section was installed in a flow rig, driven by a downstream vacuum pump system, while an upstream nitrogen bottle fed the working fluid to the probe through a flowmeter and controller. At the ends of the test section, two stagnation chambers were located and a valve manifold was installed in front of the pumps. A sketch of the test rig is shown in figure 1.

Two Brooks flowmeters and controllers were adopted for measures in the range 0.1–200 sccm (with an accuracy of 2.4 % of minimum reading.). We recall that 1 sccm (standard cubic centimetre per minute) corresponds to 1.92×10^{-8} Kg s^{-1} for nitrogen. The pressure was measured by MKS-672 absolute manometers (with range $10^{-4} - 10^3$ mbar and an accuracy of 0.12 % of minimum reading) and by a MKS-223 Baratron differential pressure gauge with range $10^{-3} - 10$ mbar and an accuracy of 0.3 % of minimum reading). An assigned flow rate Q could be established through the test section, by operating on the flowmeter and controller, while the pressure in the downstream stagnation chamber was controlled by the valve manifold.
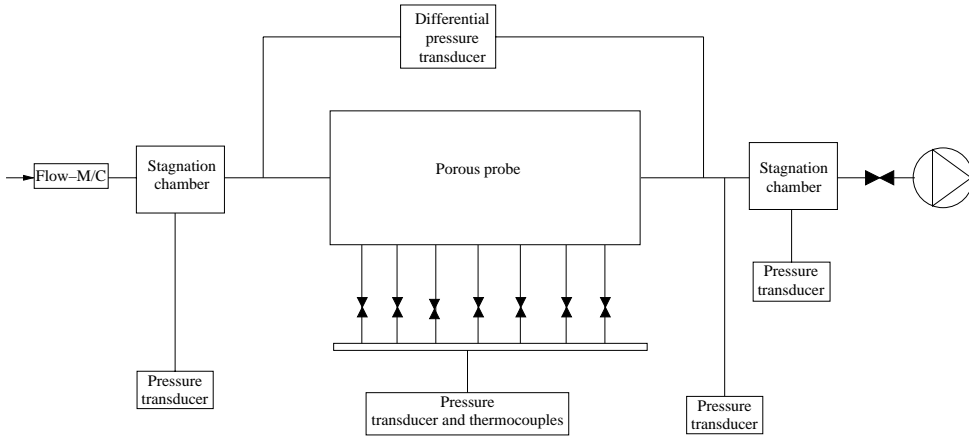
FIGURE 1. Sketch of the experimental set-up.

The J-type thermocouples measured the temperature inside the bed of spheres. In all the experiments, the temperature T measurements showed that the flow was practically isothermal, with temperature variations of less than one K with respect to the external temperature.

Two typical sets of data are reported in figure 2 and show the measured wall pressure distribution in the axial direction x, made dimensionless with respect to L. Experiments carried out in the past measured the drop in gas pressure between the inlet and the outlet of a test section, and led to the evaluation of an average permeability over the total length L of the probe $\bar{K}_d = u p_{av}/(|\Delta p/L|)$, where $p_{av} = (p_{in} + p_{out})/2$ and $\Delta p = (p_{in} - p_{out})$. Therefore the influence of the end effects on the results was not taken into account and, moreover, the extent of possible comparisons with mathematical models was limited. In our case, the local value of the permeability could be calculated – with good accuracy – from the distribution of the local pressure values. In addition, operating at a constant flow rate in isothermal conditions provided a means for a relatively immediate evaluation of the velocity distribution along the test section.

As an anticipation to the presentation of the numerical simulations, the wall pressure and the pressure at the centreline are also shown in figure 2, as calculated by a code based on a direct simulation Monte Carlo method (DSMC) to be discussed later. The graphs refer to two cases corresponding to two parameters, namely Kn_i and Re_i. Here, $Kn_i = \lambda_i/d_p$ and $Re_i = \rho_i u_i d_p/\mu$ are the Knudsen number and the Reynolds number, respectively, and the index i stands for inlet conditions. Moreover, λ is the gas mean free path and then assuming isothermal conditions for the flow, leads to a constant value of the Reynolds number, along the probe. In both cases, the Mach number $Ma = u/c$, where c is the speed of sound, was very small.

We note that the pressure distribution *vs.* x is not linear at the higher Kn_i, while, at the lower Kn_i, i.e. in a more although not yet continuous situation, the p *vs.* x relation becomes almost linear. Furthermore, we already observe at this point that the mathematical model provides a good representation of the experiments in both cases and that the small difference between the values calculated at the wall and those along the centreline increases with Kn_i. Testing the simulation results against the experimental data helps validate the model and allows us to make an estimate of the pressure values along the axis from those along the external wall.
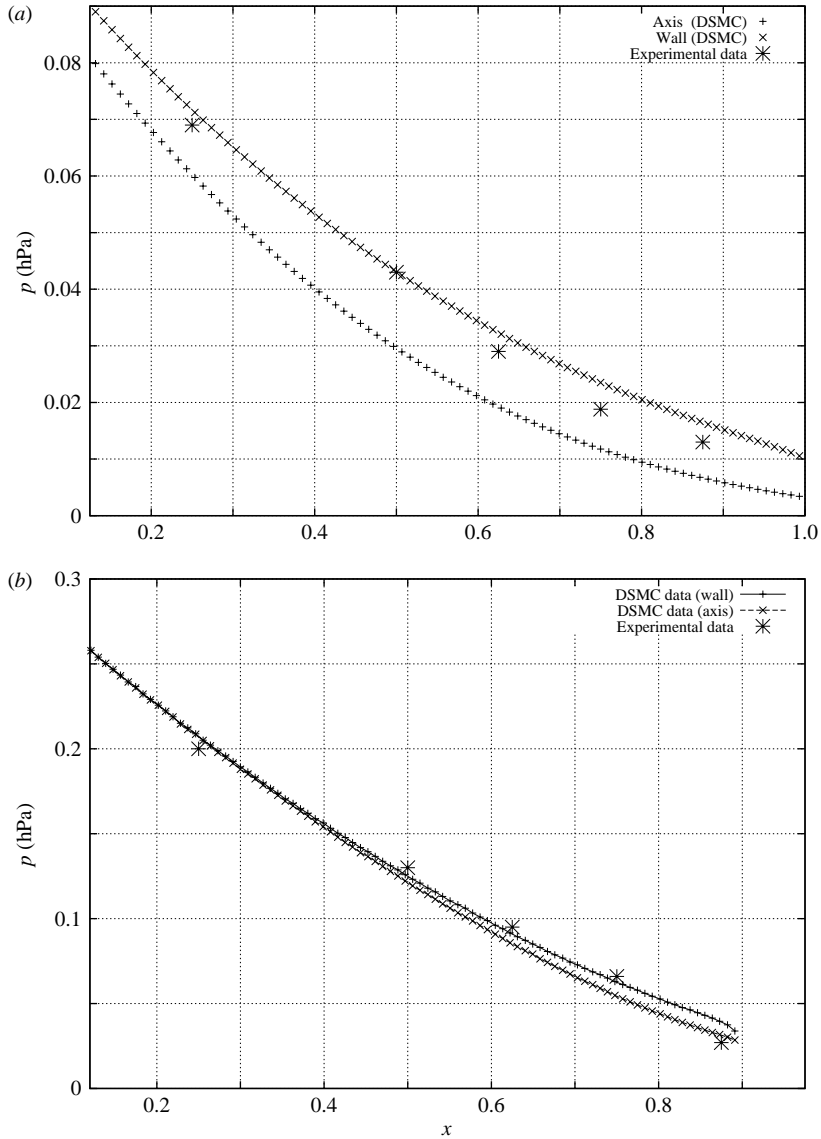
FIGURE 2. Experimental and simulated pressure distributions p along the longitudinal axis x at different Knudsen numbers at the inlet and flow rates. (a) $Kn_i = 1.05$, $Re_i = 1.4 \times 10^{-2}$. (b) $Kn_i = 0.2$, $Re_i = 5.78 \times 10^{-2}$.

After running a set of experiments in a range of Kn_i and Re_i, data such as those in figure 3 were obtained. In particular, the figure shows the local Kn^{-1} *vs.* x distribution. The data are relative to three different values of $D_s/D_w (1.85 \times 10^{-2}, 3.7 \times 10^{-2}, 7.4 \times 10^{-2})$ and three values of Re_i and the influence of the ratio D_s/D_w on the results increases with the rarefaction, but is negligible in percentage.

The local permeability $K_d = up/(|\nabla p|)$ was calculated from the experimental data by interpolating the pressure values along x, and was made dimensionless with respect to the reference $K_r = \sqrt{RT} D_s$, where R is the gas constant. Figure 4 shows K_d/K_r as a function of Kn^{-1} and Kn, with figure 4(a) reporting the experimental data in the
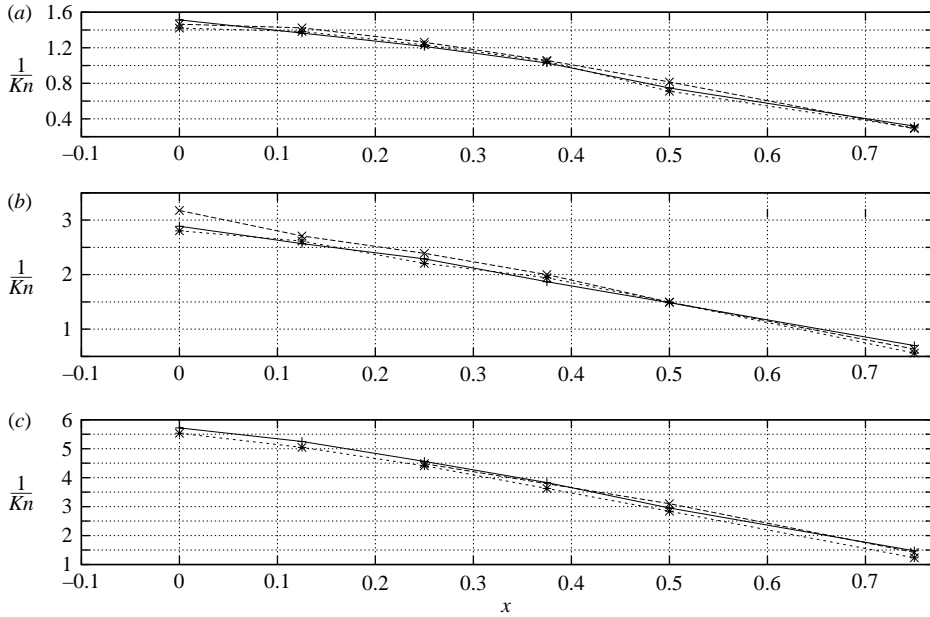
FIGURE 3. $1/Kn$ distributions along the longitudinal axis x at different diameters of the spheres D_s and flow rates Q. Experimental data. (a) $Q = 0.25\,\text{sccm}\,(Re_i = 1.4 \times 10^{-2})$; (b) $Q = 0.5\,\text{sccm}\,(Re_i = 2.8 \times 10^{-2})$; (c) $Q = 1\,\text{sccm}\,(Re_i = 5.78 \times 10^{-2})$. —, $D_s = 0.5\,\text{mm}$; $\times$, $1.0\,\text{mm}$; *, $2.0\,\text{mm}$.

entire range of Kn values, for $Re_i = 1.4 \times 10^{-2}$–5.78, together with a best fit curve (dashed line). As a first preliminary result of this work the enlarged representation in figure 4(b) shows the clear presence of a minimum at Kn about 6. This result provides an answer to the controversial results in the literature and shows that such a minimum exists at least in beds of equal diameter spheres.

A second result concerns the Klinkenberg effect and figure 5 shows the experimental data obtained in the almost continous range for $Kn_i = 7.6 \times 10^{-3} - 3.4 \times 10^{-2}$, and $Re_i = 5.78 - 0.578$ and a best fit dashed line is also given. When reference is made to the Darcy equation for a continuum flow in the form of (1.2), and to the Klinkenberg law (1.5), our experiments show that the permeability can be given the expression $k = 3.87 \times 10^{-10}(1 + 184/p_{av})$, (SI units), which extend the results of the models for the continuum regime (Wu *et al.* 1998; Chastanet *et al.* 2004). Moreover, Marschall & Milos (1998) presented experimental results for flows through rigid fibrous matrices in a range of Kn between 0.1 and 1. In their case, values of b about $703 - 877\,\text{Pa}$ were obtained whose order of magnitude approximately compares with that of our experiments with a bed of spheres in spite of the relevant differences of materials and flow regimes.

3. Physical model and numerical computations

The model proposed in this paper assumes that the particles crossing the medium proceed while either colliding or not colliding against the spheres. A fraction β of the total number of molecules in each volume element strikes the spheres and a fraction $(1 - \beta)$ does not. In the second case, they possibly collide with other particles. In
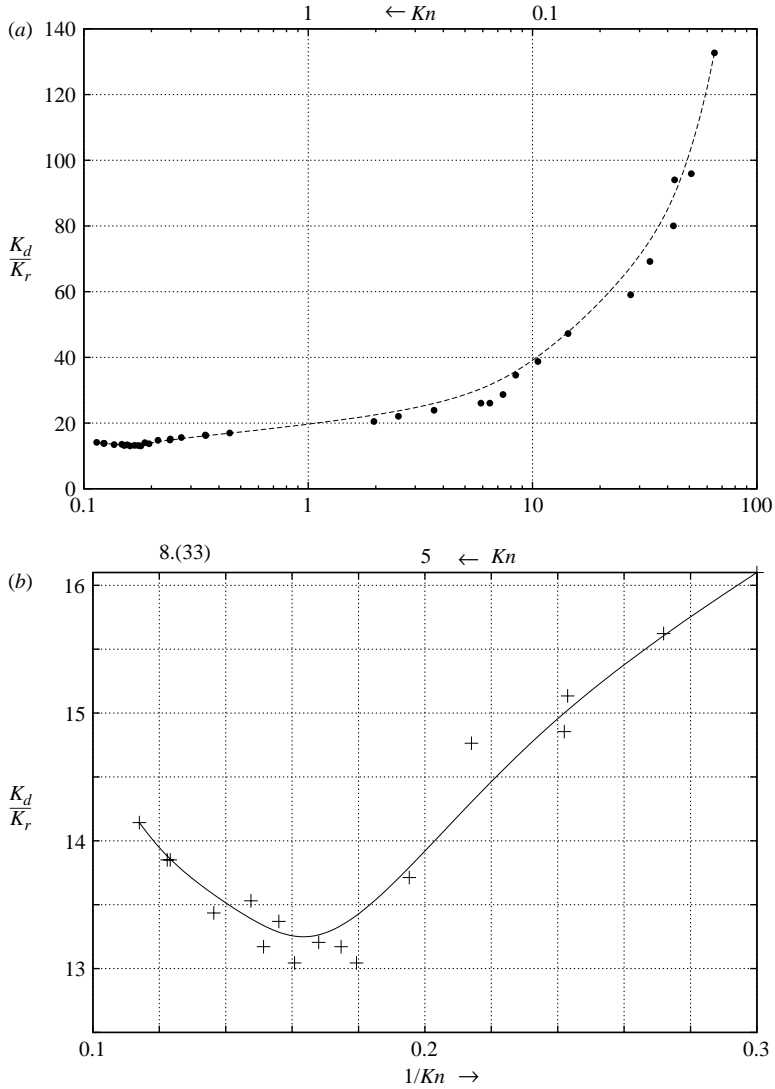
FIGURE 4. Dimensionless permeability K_d/K_r $vs.$ Kn^{-1}, $Re_i = 1.4 \times 10^{-2}-5.78$.

both cases, they can hit the external wall if the proper conditions are verified. The two types of collision depend upon the geometry of the matrix (porosity, tortuosity of the flow path) and on the characteristics of the interaction between gas and solid.

Our approach somehow recalls that proposed by Erofeev *et al.* (1995) and Plotnikov & Rebrov (2003) who evaluated the hypersonic flow against an infinitely thin permeable membrane by a DSMC procedure. In their work, the gas molecules striking the permeable surface are either rejected or pass through according to an assumed probability.

The numerical simulations and the computations were carried out according to the DSMC method which is a well-established numerical approach for the analysis of gas dynamics phenomena at a molecular level (Bird 1994; Alexander & Garcia 1997). The microscopic state of the system is defined by the position $\boldsymbol{x}(x, y, z)$ and velocity

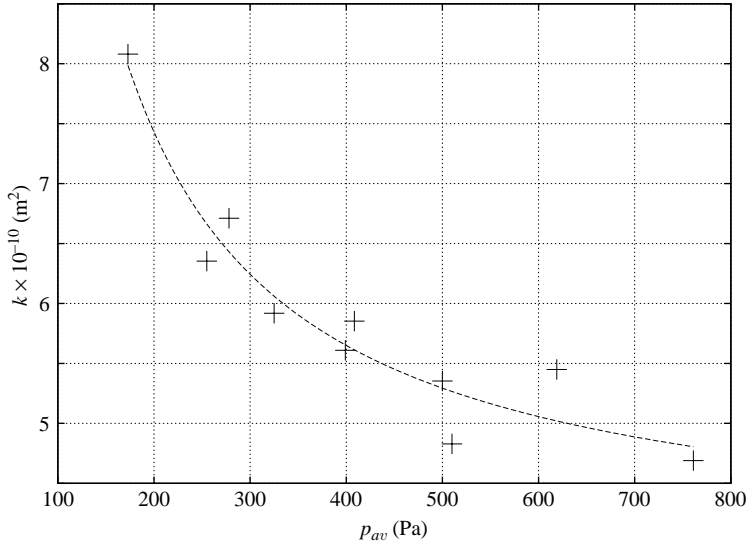FIGURE 5. Experimental Klinkenberg's law, dimensional units.
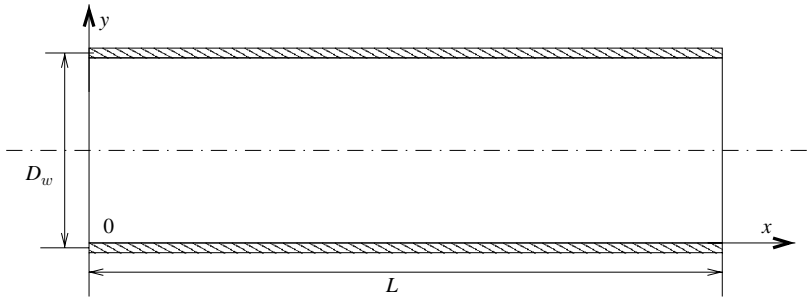

FIGURE 6. Geometry of the problem.

$u'(u', v', w')$ of a set of representative particles which move in the physical domain. All the flows are computed as unsteady while the physical time is the parameter of the simulation.

One of the most important aspects of the DSMC is to uncouple the molecular motion from the intermolecular collisions. In particular, the physical domain is discretized in cells, and during each time step the particles move in each cell and through its borders under the proper boundary conditions and collide following a stochastic process where momentum and energy are invariants. At the end of each step, a new macroscopic state of the system (T, p, ρ, u) is evaluated from the microscopic state of each cell according to the laws of the classical kinetic theory (Bird 1994). A few physical definitions and data are given in the Appendix.

The DSMC code simulates the two-dimensional flow in a cylindrical region where a system of coordinates $(0xy)$ represents the axial (x) and radial (y) directions, respectively, and the origin 0 is on the wall. Figure 6 reports a sketch of the geometry. The distance y from the wall is made dimensionless with respect to the probe radius $D_w/2$ while the reference length along x is L and the two-dimensional domain is discretized in $N_x \times N_y$ cells.
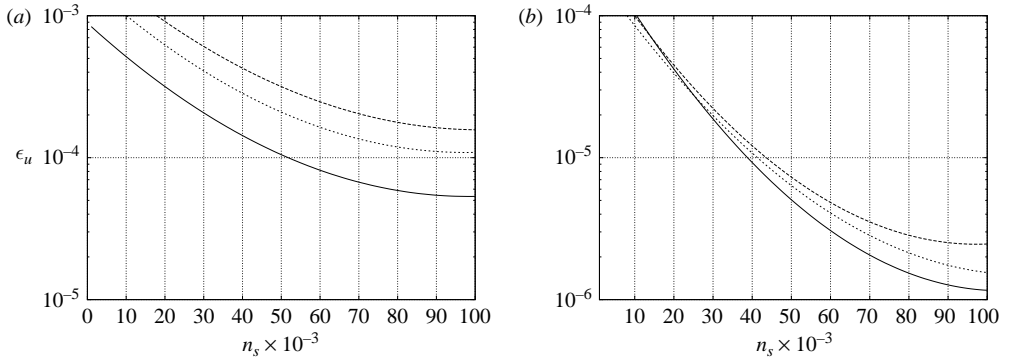
FIGURE 7. Rate of convergence of (*a*) the macroscopic velocity and (*b*) number density *vs.* the number of steps. (i) ——, $N_{tot} = 1500$, $n_m = 10^6$; (ii) - - - -, $N_{tot} = 1500$, $n_m = 10^5$; (iii) $\cdots$, $N_{tot} = 6000$, $n_m = 10^6$.

The numerical program was then run after assuming that the nitrogen molecules enter the tube at the pressure p and temperature T which correspond to the experimental data at the inlet, while the pressure at the outlet is also assigned from the experiments. The procedure adopted to assign these boundary conditions follows the analysis presented by Wu *et al.* (2001). In particular, an iterative algorithm is followed to calculate the streamwise component of the velocity which satisfies the conservation of the particle fluxes both at the inlet and at the outlet boundary surfaces. As an alternative it is possible to specify the mass flow rate and the exit pressure. The two different choices are equivalent as they give the same flow properties all over the domain and the details of the iterative procedure are given in Wu *et al.* (2001).

We recall that the main numerical parameters involved in each DSMC run are the number $N_{tot} = N_x \times N_y$ of cells adopted, the number of representative molecules n_m used in the simulation, and the number of steps n_s which are necessary to reach the numerical convergence. Each representative molecule corresponds to a random sample, drawn from the actual velocity distribution, of the usually very large number of real molecules (Alexander & Garcia 1997; Bird 1998). The optimum choice of the parameters above is not immediate but depends upon the particular problem which is investigated. Some suggestions can be inferred from the behaviour of the norm of a significant macroscopic quantity (e.g. the number density n, the mean velocity u or the temperature T) in a particular cell or in a group of cells. More details can be found in de Socio & Marino (2000) where this criterion was introduced. In the present calculations we assumed as references quantities $\epsilon_u = |u_i - u_{i-1}|/|u_i|$ and $\epsilon_n = |n_i - n_{i-1}|/n_i$, evaluated in the cell at $x = 0.5$, $y = 1$. The subscript i represents the current step.

Figure 7 shows ϵ_u and ϵ_n as functions of three parameters N_{tot}, n_s and n_m, and we note that the rates of convergence of ϵ_u and ϵ_n *vs.* n_s increase more rapidly with n_m than with N_{tot}.

By following this procedure, very good accuracy and convergence were obtained by means of $N_{tot} = 50 \times 30$ computational cells and $n_m = 10^6$ representative molecules. Moreover 10 000 steps were sufficient to achieve numerical convergence, with ϵ_n and ϵ_u both less than 10^{-4}. The curves also confirm that the error in a Monte Carlo simulation is proportional to $1/\sqrt{n_m}$ (Hadjiconstantinou *et al.* 2003).
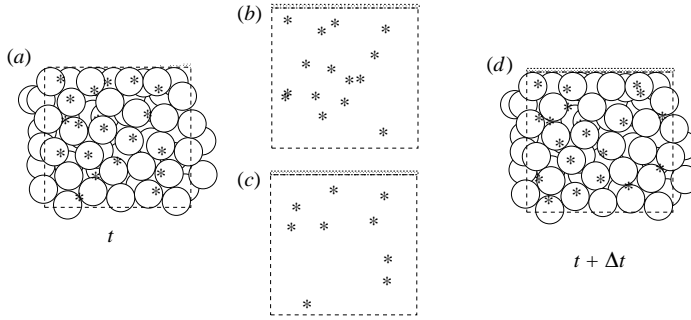
FIGURE 8. Sketch of the physical model for the gas flow through a bed of spheres.

To explain the assumptions better, figure 8 shows a sketch of the model. Figure 8(*a*) shows, at time *t*, a discrete volume element $\Delta\Omega$ of the material close to an element of the external wall $\partial\Omega$ and a few representative gas particles n_m are shown as stars. The problem of the collisions between gas particles and spheres is then split in two parts. The surfaces of the spheres are considered in figure 8(*b*) as homogeneously distributed in the domain $\Delta\Omega$ where a fraction β of the n_m representative particles is trapped. Whatever the kinetic state of these particles may be, they lose their energy against the distributed wall and gain a new kinetic state according to a Maxwellian distribution function at the temperature of the wall in $\Delta\Omega$. The remaining $(1-\beta)n_m$ representative molecules move freely in the space $\Delta\Omega$ (figure 8*c*) and may collide according to the usual rules which take into account their relative speed, the collision cross-section and so on. Possible collisions against the wall $\partial\Omega$ are treated following the usual rules and the impinging molecules are diffusely re-emitted. Figure 8(*d*) refers to the updated microscopic state at $t+\Delta t$.

For a compact bed of spheres, the geometric properties are well known and we also observed, during our work, that small variations of these characteristics do not particularly affect the final results. Moreover, we assume that the probe is isothermal and that the colliding molecules are re-emitted according to a Maxwellian distribution function at the constant temperature of the spheres. We assume that the local flow through the pores occurs as through a long microtube at the same Kn value. Analogously to the Pollard & Present (1948) and Scott & Dullien (1962) approach to the flow through capillaries, the fraction of molecules β which arrive, on average, from the wall of spheres directly onto a sphere without encounters with other molecules is

$$\beta = \exp[-\sinh^{-1}(Kn^{-1})]. \tag{3.1}$$

In the case of a permeable medium, Kn is evaluated as a function of the location in each run.

At each calculation step, the representative molecules in an elemental cell are sorted from the total number according to the local β value of (3.1) and then this β fraction is assigned a velocity value from a random Maxwellian distribution at the constant temperature T. Proper care is paid to the fact that the molecules impinging on the external wall are re-emitted in a solid angle 2π while those colliding with the spheres are re-emitted in all directions. Moreover the sorted fraction $1-\beta$ of the total number of molecules in each cell is dealt with according to the collision laws for hard spheres in an empty space following a standard Monte Carlo procedure. The microscopic state at $t+\Delta t$ in $\Delta\Omega$ comes out from the microscopic state of all particles which are
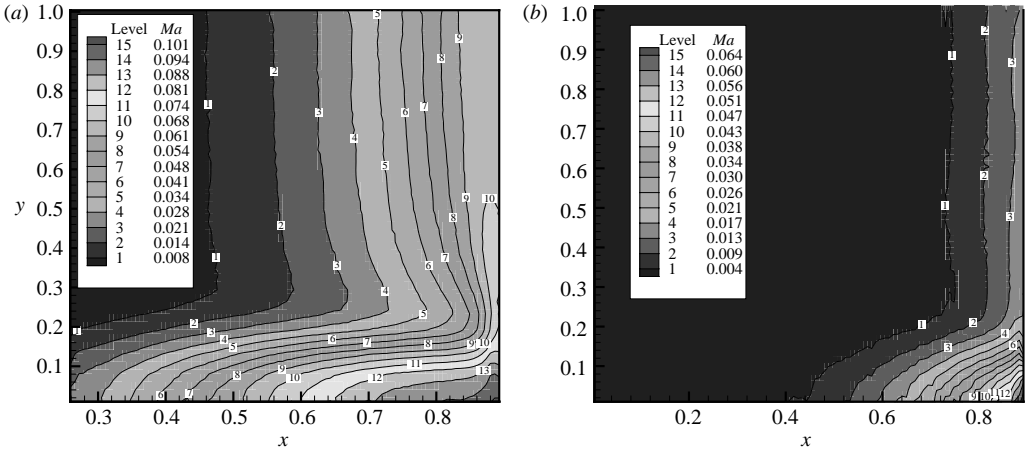
FIGURE 9. Two-dimensional Mach number distributions. y = dimensionless distance from the wall. (*a*) $Kn_i = 1.05$, $Re_i = 1.4 \times 10^{-2}$. (*b*) $Kn_i = 0.2$, $Re_i = 5.78 \times 10^{-2}$.
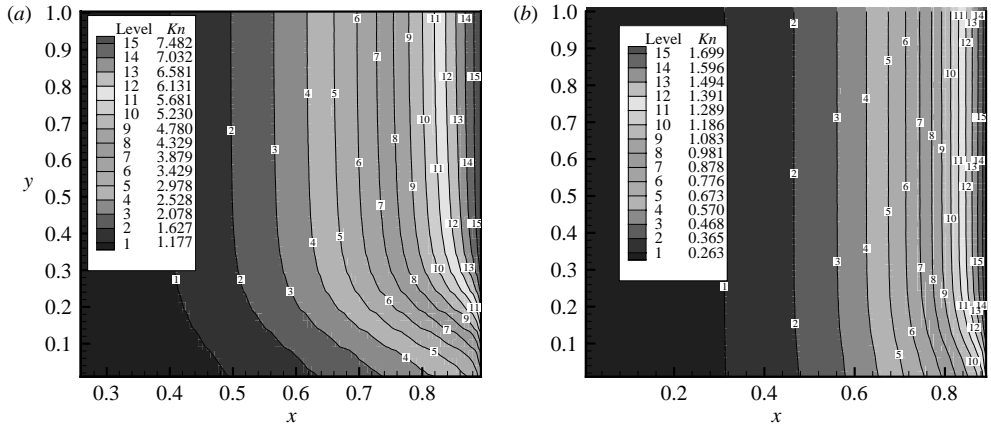
FIGURE 10. Two-dimensional Knudsen number distributions. y = dimensionless distance from the wall. (*a*) $Kn_i = 1.05$, $Re_i = 1.4 \times 10^{-2}$. (*b*) $Kn_i = 0.2$, $Re_i = 5.78 \times 10^{-2}$.

in the volume element at $t + \Delta t$. Details on this particular point follow the lines in Bird (1994).

The computations were carried out for Re_i ranging between 1.4×10^{-2} and 5.78 and for Kn_i between 7.6×10^{-3} and 1.05. In this range of Kn_i, the local values of Kn could be as high as 10. We have already shown, in the preceding section, the excellent agreement between simulated and experimental data at relatively high Kn_i. Now turning back to figure 2, we note that the difference between calculated values and experimental data increases with x through the local value of $Kn(x)$.

As we have already said, a boundary layer is present along the cylindrical wall and the results of the simulations for the two cases in figure 2 are reported in figures 9 and 10. There the distributions of the local Ma and Kn values close to the cylindrical wall are reported after calculating the local values of β from (3.1). The boundary-layer thickness is a negligible fraction of the probe radius $D_w/2$. Correspondingly, the changes of porosity at the wall and at the ends of the tube are negligible.
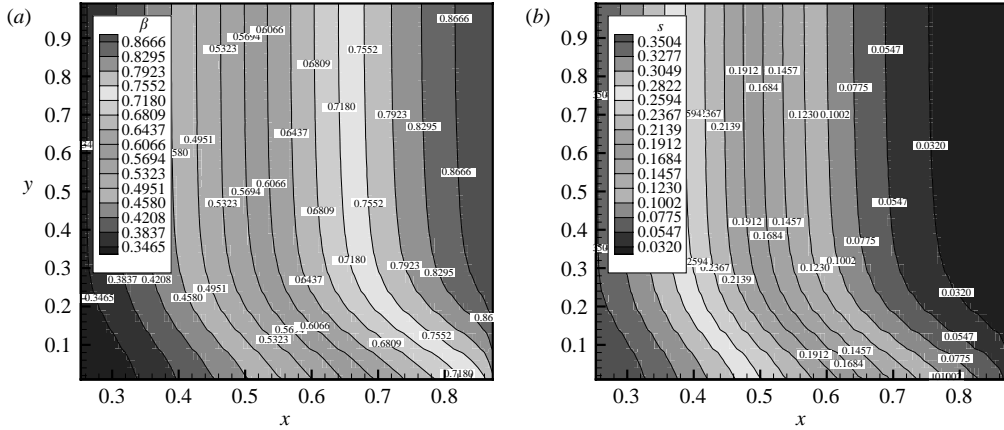
FIGURE 11. Two-dimensional (*a*) β and (*b*) s distributions. y = dimensionless distance from the wall. $Kn_i = 1.05$, $Re_i = 1.4 \times 10^{-2}$.
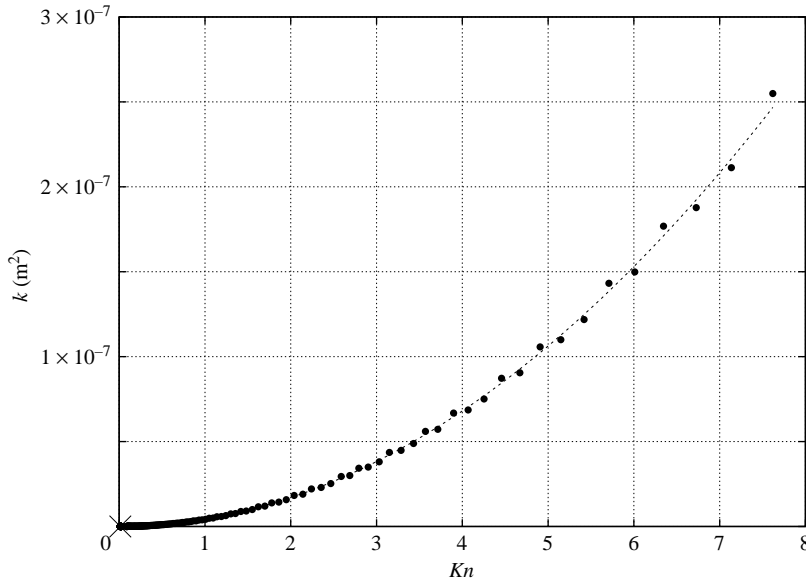

FIGURE 12. Permeability k distribution *vs*. the local Kn.

We finally calculated some cases for values of β constant in each run and equal to the value which in each situation corresponds to the value of Kn in the centreline at the exit. The errors between calculated and experimental data were, in both cases, less than a few per cent and showed that the sensitivity of the thermo-fluid-dynamical state to β

$$s = \mathrm{d}\beta/\mathrm{d}Kn = \exp[-\sinh^{-1}(Kn^{-1})]/(Kn^2\sqrt{1 + 1/Kn^2}), \qquad (3.2)$$

is negligible, at least in a range of flow regimes from the free molecular up to the transitional flows. The β distribution near the wall in a significant case is shown in figure 11(*a*) while the corresponding sensitivity is given in figure 11(*b*).

From all the simulations, the permeability $k(Kn)$ was obtained in a range of Knudsen number and is reported in figure 12. A best fitting (dashed line) of the

numerical data for Kn between 0.01 and 8.0 gives $k\,[\mathrm{m}^2] = 4.25 \times 10^{-9}(Kn^2)$. For Kn between 0.2 and 2.0, the experimental data from figure 5 fall on this curve.

4. Conclusions

After presenting the results of our experiments and numerical simulations we conclude with a few observations. The number of works which concern the flow of fluids through porous media is extremely great. This is due, on one hand, to the large number of applications and, on the other hand, to the intrinsic interest of their physics and mathematical models. However, very few papers approach the flows through permeable media with reference the molecular gasdynamics. This happened, for instance, only recently in evaluating the velocity slip between gas and solid, or in justifying the presence of nonlinear terms in extended forms of the Darcy equation. In any case, the privileged point of view of all investigations remained that of continuum fluid mechanics, although interest in gas flow through the microchannels of a permeable medium is increasing. It seemed then worth making a first contribution to the study of the problem by some experimental technique and classical procedure of molecular kinetics. We proposed a simple mathematical model for a bed of spheres which is one of the most representative examples of permeable medium and the one that is most suitable for a statistical representation of its geometric characteristics.

In particular, we dealt with a problem where the Knudsen number, evaluated on a microscopic basis, is such that the flow regimes fall between the free molecular flow and the transition regime, whereas the macroscopic Knudsen-number value corresponds to a continuum fluid. The model and its Monte Carlo simulations were validated against the experimental data and proved the viability of the kinetic approach and the efficiency of the numerical method. Among the results are an extension of the existing theories of the medium permeability to gas flows, the proof that an effect analogous to the Knudsen effect in tubes exists also in a bed of spheres, and a general expression for the Klinkenberg law for a permeable medium.

Appendix. Physical definitions and data

A few definitions and figures are recalled which were adopted in the experimental data reduction and in the numerical simulations.

The microscopic state of the nitrogen gas is described by a hard sphere model for its molecules of mass $m = 46.5 \times 10^{-27}$ kg, mean collision diameter $\bar{d} = 4.17 \times 10^{-10}$ m and velocity $\boldsymbol{u}'(u', v', w')$.

The mean thermal speed is given by $\overline{c'^2} = (\overline{u'^2} + \overline{v'^2} + \overline{w'^2})$ and the mean free path $\lambda = \overline{c'}/\bar{v}$ where $\bar{v}$ is the mean collision frequency.

In a equilibrium hard sphere gas $\lambda = 1/\sqrt{2}\pi\bar{d}^2 n$ where n is the number density.

Since $\overline{c'^2} = 3kT/m$, where the Boltzmann constant $k = 1.38 \times 10^{-23}$ J K^{-1}, defines the temperature T, the equation of state gives the pressure $p = nkT$. Furthermore, the viscosity μ was calculated by means of $\mu = (5/16)\sqrt{RT/\pi m}/\bar{d}^2$ where the gas constant was taken as $R = 196.77$ J K^{-1} Kg^{-1}.

REFERENCES

Adzumi, H. 1937*a* Studies on the flow of gaseous mixtures through capillaries: I. The viscosity of binary gaseous mixture. *Bull. Chem. Soc. Japan* **12**, 199–226.

ADZUMI, H. 1937*b* Studies on the flow of gaseous mixtures through capillaries: II. The molecular flow of gaseous mixtures. *Bull. Chem. Soc. Japan* **12**, 285–291.

ALEXANDER, F. J., GARCIA, A. L. 1997 The direct simulation Monte Carlo method. *Comput. Phys.* **11**, 588–593.

BEAR, J. 1988 *Dynamics of Fluids in Porous Media*. Dover.

BIRD, G. A. 1994 *Molecular Gas Dynamics and Direct Simulation of Gas Flows*. Oxford University Press.

BIRD, G. A. 1998 Recent advances and current challenges for DSMC. *Comput. Maths Applic.* **35**, 1–14.

CHAMBERS, A. 2005 *Modern Vacuum Physics*. Chapman & Hall.

CHASTANET, J., ROYER, P., AURIAULT, J.-L. 2004 Does Klinkenberg's law survive upscaling? *Trans. Porous Media* **56**, 171–198.

DERJAGIN, B. B. & BAKANOV, S. P. 1957 Theory of gas flow in a porous body near the Knudsen region. Pseudomolecular flow. *Sov. Phys. Dokl.* **2**, 326–331.

DULLIEN, F. A. L. 1991 *Porous Media, Fluid Transport and Porous Structure*, 2nd edn. Academic.

EROFEEV, A. I., FREEDLENDER, O. G. & KOGAN, M. N. 1998*a* Rarefied gas condensation by a porous layer. In *Proc. 21st Intl Symp. on Rarefied Gas Dynamics*, pp. 495–501. Cépaduès-Editions.

EROFEEV, A. I., FREEDLENDER, O. G. & KOGAN, M. N. 1998*b* Rarefied gas flow through a porous layer. In *Proc. 21st Intl Symp. on Rarefied Gas Dynamics*, pp. 639–646. Cépaduès-Editions.

EROFEEV, A. I., FREEDLENDER, O. G., PERMINOV, V. D. & SVISCHEV, S. V. 1995 Hypersonic rarefied gas flow over a porous plate. In *Proc. 19th Intl Symp. on Rarefied Gas Dynamics*, vol. 2, pp. 1263–1269. Oxford University Press.

GORELIK, G., PAYLYUKEVICH, N., ZALENSKIY, S., RADEV, S. & STEFANOV, S. 1993 Kinetics of intense evaporative mass transfer through a porous layer. *Intl J. Heat Mass Transfer* **36**, 3369–3374.

GROVE, D. M. & FORD M. G. 1958 Evidence for permeability minima in low-pressure gas flow through porous media. *Nature* **182**, 999–1000.

HADJICONSTANTINOU, N. G., GARCIA, A. L., BAZANT, M. Z. & HE, G. 2003 Statistical error in particle simulations of hydrodynamic phenomena. *J. Comput. Phys.* **187**, 274–297.

KARNIADAKIS, G. M. & BESKOK A. 2001 *Micro Flows*. Springer.

KLINKENBERG, L. J. 1941 The permeability of porous media to liquid and gases. *Drilling and Production Practice*, pp. 200–213. American Petroleum Inst.

KNUDSEN, M. 1909 Die Gesetze der Molekularströmung und der innern Reibungsströmung der Gase durch Röhren. *Annln Phys.* **28**, 75–130.

MARSCHALL, J. & MILOS, F. S. 1998 Gas permeability of rigid fibrous refractory insulations. *J. Thermophys. Heat Transfer* **12**, 528–535.

MUSKAT, M. 1937 *The Flow of Homogeneous Fluids through Porous Media*. McGraw–Hill.

PLOTNIKOV, M. YU & REBROV, A. K. 2003 Supersonic flow through a permeable obstacle. In *AIP Conf. Proc. 23rd Intl Symp. on Rarefied Gas Dynamics*, vol. 663 (ed. A. D. Ketsdever & E. P. Muntz), pp. 157–163, Melville, New York.

POLLARD, W. G. & PRESENT, R. D. 1948 On gaseous self-diffusion in long capillary tubes. *Phys. Rev.* **73**, 762–774.

SCOTT, D. S. & DULLIEN, F. A. L. 1962 The flow of rarefied gases. *A.I.Ch.E. J.* **8**, 293–297.

SKJETNE, E. & AURIAULT, J.-L. 1999 Homogenization of wall slip in the Darcy flow through porous media. *Trans. Porous Media.* **36**, 293–306.

DE SOCIO, L. M. & MARINO, L. 2000 Numerical experiments on the gas flow between rotating cylinders. *Intl J. Numer. Meth. Fluids* **34**, 229–240.

STEFANOV, S., FREZZOTTI, A., LEVDANSKY, V. LEITSINA, V. & PAYLYUKEVICH, N. 1999 Direct statistical simulation of gas mixture mass transfer in a porous layer with condensation of one of the components and adsorption of another. *Intl J. Heat Mass Transfer* **42**, 2063–2069.

WICKE, E. & VOLLMER, W. 1952 Flow of gases through micropores. *Chem. Engng Sci.* **1**, 282–291.

WU, J.-S, LEE, W.-S, LEE, F. & WONG, S.-C. 2001 Pressure boundary treatment in internal gas flow at subsonic speed using the DSMC method. In *Rarefied Gas Dynamics: Proc. 22nd Intl Symp.* (ed. T. J. Bartel & M. A. Gallis), vol. 585, pp. 408–416. American Institute of Physics.

WU, Y. S., PRUESS, K. & PERSOFF, P. 1998 Gas flow in porous media with Klinkenberg effects. *Trans. Porous Media* **32**, 117–137.